Beyond the Proton Abstracting Role of Glu-376 in Medium-Chain Acyl-CoA Dehydrogenase: Influence of Glu-376→Gln Substitution on Ligand Binding and Catalysis†

K. V. Gopalan and D. K. Srivastava*

Department of Biochemistry and Molecular Biology, North Dakota State University, Fargo, North Dakota 58105

Received August 16, 2001; Revised Manuscript Received February 12, 2002

ABSTRACT: The active site residue, Glu-376, of medium-chain acyl-CoA dehydrogenase (MCAD) has been known to abstract the α-proton from acyl-CoA substrates during the course of the reductive half-reaction. The site-specific mutation of Glu-376→Gln(E376Q) slows down the octanoyl-CoA-dependent reductive half-reaction of the enzyme by about 5 orders of magnitude due to impairment in the proton-transfer step. To test whether the carboxyl group of Glu-376 *exclusively* serves as the active site base (for abstracting the α-proton) during the enzyme catalysis, we undertook a detailed kinetic investigation of the enzyme−ligand interaction and enzyme catalysis, utilizing octanoyl-CoA/octenoyl-CoA as a physiological substrate/product pair and the wild-type and E376Q mutant enzymes as the catalysts. The transient kinetic data revealed that the E376Q mutation not only impaired the rate of octanoyl-CoA-dependent reduction of the enzyme-bound FAD, but also impaired the association and dissociation rates for the binding of the reaction product, octenoyl-CoA. Besides, the E376Q mutation correspondingly impaired the kinetic profiles for the quenching of the intrinsic protein fluorescence during the course of the above diverse (i.e., "chemistry" versus "physical interaction") processes. A cumulative account of the experimental data led to the suggestion that the carboxyl group of Glu-376 of MCAD is intimately involved in modulating the microscopic environment (protein conformation) of the enzyme's active site during the course of ligand binding and catalysis. Arguments are presented that the electrostatic interactions among Glu-376, FAD, and CoA-ligands are responsible for structuring the enzyme's active site cavity in the ground and transition states of the enzyme during the above physicochemical processes.

The medium-chain acyl-CoA dehydrogenase (MCAD)[1] catalyzed reaction proceeds via abstraction of the *pro-R* α-proton from acyl-CoA substrate by the enzyme's active site residue, Glu-376, with concerted transfer of the *β*-hydrogen (in the form of hydride) to the N5 position of the isoalloxazine ring of the enzyme-bound FAD (for reviews, see *1*−*3*). A combination of these steps results in the formation of the two-electron-reduced flavin ($FADH_2$) and the corresponding enoyl-CoA product. The step involved in the binding of acyl-CoA, followed by the reduction of the enzyme-bound FAD with concomitant oxidation of acyl-CoA to enoyl-CoA, is conventionally referred to as the reductive half-reaction of the enzyme (Scheme 1).

Scheme 1

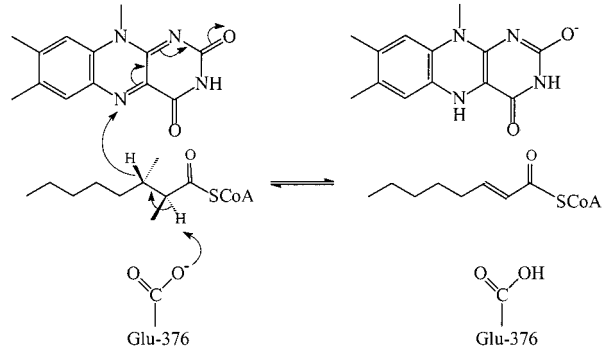

One of the most interesting aspects of MCAD catalysis is the marked similarity in the microscopic pathways for the octanoyl-CoA-dependent reductive half-reaction and the binding of the reaction product, octenoyl-CoA, to the enzyme's active site. Kumar and Srivastava (*4*, *7*) first demonstrated that the transient kinetic profiles for the octanoyl-CoA-dependent reduction of the pig kidney enzyme-bound FAD were precisely the same (both qualitatively as well as quantitatively) as the octenoyl-CoA-dependent changes in the electronic structure of the enzyme-bound FAD. A similar conclusion was discerned for the binding/reactivity of the above ligands with the recombinant form of human liver MCAD (*5*). In the latter studies, Peterson et al. provided evidence that the above similarity was also extended to the binding of another C_8-CoA ligand, namely, octynoyl-CoA, a mechanism-based inactivator of the enzyme (*5*). The origin of the above similarity was ascribed to the

† This work was supported by National Science Foundation Grant MCB-9904416.

* To whom correspondence should be addressed at the Department of Biochemistry and Molecular Biology, North Dakota State University, Fargo, ND 58105. Tel: (701) 231-7831. Fax: (701) 231-9657. Email: dk.srivastava@ndsu.nodak.edu.

[1] Abbreviations: MCAD, medium-chain acyl-CoA dehydrogenase; FAD, flavin adenine dinucleotide; $FcPF_6$, ferricenium hexafluorophosphate; K_c, dissociation constant of the collision complex; EDTA, ethylenediaminetetraacetic acid; C_8-CoA, octanoyl-CoA, octenoyl-CoA, or octynoyl-CoA.

10.1021/bi011676p CCC: $22.00 © 2002 American Chemical Society
Published on Web 03/14/2002

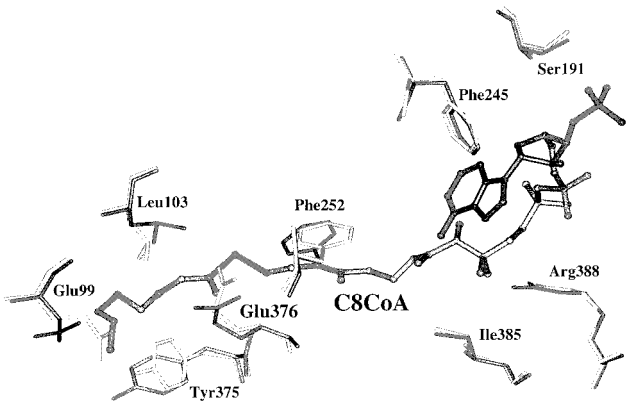

FIGURE 1: Spatial relationship of selected amino acyl residues in the vicinity (within 4 Å perimeter) of the enzyme-bound C_8-CoA. The selected amino acyl residues have been derived from the X-ray crystallographic data of pig liver medium-chain acyl-CoA dehydrogenase in the absence (light shade) and presence of C_8-CoA (dark shade). Note the swinging of the carboxyl group of Glu-376, from its original position in the ligand-free ("apo") structure of the enzyme upon binding octenoyl-CoA ("holo" structure).

coupling between the protein conformational and ligand structural changes (*4*, *5*). In the case of octanoyl-CoA, it was manifested in the form of the chemical transformation of octanoyl-CoA to octenoyl-CoA, whereas in the cases of octenoyl-CoA and octynoyl-CoA, it simply involved the changes in the electronic structures of the interacting species (*4*).

It has been demonstrated that the binding of a variety of CoA-ligands to MCAD proceeded at least via a "two-step" mechanism (eq 1; *12*−*16*).

$$\text{MCAD} + \text{ligand} \underset{K_c}{\rightleftharpoons} \text{MCAD}-\text{ligand} \overset{k_f}{\underset{k_r}{\rightleftharpoons}} (\text{MCAD}-\text{ligand})^* \quad (1)$$

The first (fast) step involved the formation of an MCAD−ligand collision complex (with a dissociation constant of K_c), in which the electronic structures of both enzyme-bound FAD and ligand remained unchanged (the "colorless" complex), followed by a slow isomerization step (with forward and reverse rate constants of k_f and k_r, respectively), with concomitant changes in the electronic structures of the enzyme-bound species (*12*). Such a two-step binding phenomenon has been noted with a number of enzymes including several flavoenzymes (*38*−*41*). We recently realized that our transient kinetic data for the binding/reactivity of octanoyl-CoA/octenoyl-CoA could also be explained by a two (instead of three)-step model (*6*).

Although the X-ray crystallographic data of both pig and human liver MCADs in the absence and presence of CoA-ligand do not provide evidence for major changes in the protein conformation, some subtle readjustments in the side chains of certain amino acyl residues have been noticed (*9*−*11*). Figure 1 shows the location of selected amino acyl residues of the protein in the absence (light shade) and presence of C_8-CoA (dark shade) within a 4 Å perimeter of the ligand. Of these, one of the most noticeable changes is the swinging of the carboxyl group of Glu-376, from its original position in the ligand-free ("apo") structure of the enzyme upon binding octenoyl-CoA ("holo" structure). The carboxyl oxygens of Glu-376 (viz., OE1 and OE2) move 1.1 and 3.78 Å, respectively, from their original positions in the "apo" structure upon formation of the "holo" structure (*5*).

Unequivocal evidence that Glu-376 serves as an active site base came from the Glu-376→Gln substitution of the human liver enzyme, which led to a drastic reduction in the rate of enzyme catalysis (*2*, *3*). In a qualitative manner, Bross et al. (*8*) demonstrated that Glu-376→Gln substitution decelerated both the reductive half-reaction and the enzyme turnover to a level of about 0.02% of the wild-type enzyme. Such an effect of the above mutation was attributed to the inability of Gln-376 in abstracting the *pro-R* α-proton from octanoyl-CoA substrate during the reductive half-reaction. However, based on our own data that the reductive half-reaction of the enzyme was intimately coupled to the changes in the protein conformation (*4*−*7*), it was of interest to investigate as to whether the above mutation had any effect on the microscopic environment of the enzyme's active site during the course of ligand binding and catalysis. As will be shown in the subsequent section, the carboxyl group of Glu-376 is intimately involved in modulating the dynamics of the protein conformational transitions during the above processes.

MATERIALS AND METHODS

Materials. Coenzyme A was purchased from Life Science Resources. *trans*-2-Octenoic acid was purchased from Pfaltz and Bauer. All other reagents were of analytical grade.

Methods. Unless otherwise stated, all experiments were performed in 50 mM potassium phosphate, pH 7.6, containing 10% glycerol and 0.3 mM EDTA (referred to as the standard buffer throughout this paper).

All molecular biology protocols were performed as outlined by Sambrook et al. (*42*). The Glu-376→Gln(E376Q) substitution in MCAD was achieved as described by Peterson et al. (*35*). The wild-type and E376Q mutant MCADs were expressed and purified according to Peterson et al. (*5*), and routinely assayed by monitoring the reduction of ferricenium hexafluorophosphate ($FcPF_6$) at 300 nm ($\epsilon = 4.3$ mM^{-1} cm^{-1}; *17*) in a reaction mixture containing 100 μM octanoyl-CoA and 350 μM $FcPF_6$. The purified enzyme preparations had an A_{280}/A_{450} ratio of about 5. The extinction coefficient of the wild-type enzyme-bound FAD was taken to be 15.4 mM^{-1} cm^{-1} at 446 nm (*18*). Since the Glu-376→Gln substitution had no effect on the absorption of the enzyme-bound FAD at 446 nm, the extinction coefficient of the mutant enzyme was taken to be the same as that of the wild-type enzyme.

Octenoyl-CoA was prepared by the mixed anhydride method of Bernhert and Sprecher (*19*) and purified on a C_{18} reverse-phase HPLC column, equilibrated with 20 mM potassium phosphate, pH 7.0, as described by Kumar and Srivastava (*4*). All CoA-derivatives were stored as lyophilized powders at −20 °C. The extinction coefficient of octenoyl-CoA was taken to be 20.4 mM^{-1} cm^{-1} at 258 nm (*4*).

Steady-State Spectrofluorometric Studies. The excitation and emission spectra of the enzyme in the absence and presence of CoA-ligands were acquired on a Perkin-Elmer LS-50B Luminescence Spectrometer as described by Peterson et al. (*6*). For emission spectra of the enzyme's

tryptophanyl residues, the excitation wavelength was fixed at 295 nm, and a 350 nm cutoff filter was placed in the emission path (*6*).

Transient Kinetic Experiments. Single-wavelength transient kinetic experiments were performed on an Applied Photophysics SX-18 MV stopped-flow spectrophotofluorometer (optical path length 10 mm, dead time 1.3−1.5 ms). The stopped-flow could be configured either in the absorption or in the fluorescence mode by changing the position of the photomultiplier tube (right angle in the case of fluorescence measurements) with respect to the incident light (*6*).

The rate constants for the association of the ligands to the enzyme were determined by mixing the above species via the stopped-flow syringes (under pseudo-first-order conditions; [E-FAD] ≪ [ligand]), and monitoring the time-dependent absorbance changes at specific wavelengths (*4*−*6*, *31*, *32*). The rate constants for the dissociation of ligands from the enzyme's active site were determined by the acetoacetyl-CoA displacement method as described by Johnson et al. (*12*).

All the transient kinetic experiments were performed at least in triplicate, and the resultant kinetic traces were averaged prior to analyses of the data by the SX-18MV software (version 4.42) developed by Applied Photophysics. The transient kinetic traces were analyzed using the single (eq 2A) or double (eq 2B) exponential (biphasic) rate equations in the following formats:

$$A = A_0 * \exp^{(-t/\tau)} + \text{offset} \qquad (2A)$$

$$A = A_f * \exp^{(-t/\tau_f)} + A_s * \exp^{(-t/\tau_s)} + \text{offset} \qquad (2B)$$

where A is the absorbance at a given time. In eq 2A, A_0 and $1/\tau$ are the total amplitude and relaxation rate constant, respectively. In eq 2B, A_f and A_s are the amplitudes of the fast and slow phases, and $1/\tau_f$ and $1/\tau_s$ are the relaxation rate constants of the fast and slow phases, respectively.

The ligand (L) concentration-dependent relaxation kinetic data were analyzed according to either a one-step (eq 3A) or a two-step (eq 3B) binding model. In the case of the two-step binding model, the first step (i.e., the formation of the EL collision complex) was assumed to satisfy the rapid equilibrium condition (*12*), with the dissociation constant K_c. In both models, k_f and k_r are the forward and reverse rate constants, respectively. The relationships between the relaxation rate constant ($1/\tau$) and the ligand concentration (under pseudo-first-order conditions; [E] ≪ [L]) are given in eq 3 for the individual models:

one-step model:

$$E + L \underset{k_r}{\overset{k_f}{\rightleftharpoons}} EL$$

$$1/\tau = k_f[L] + k_r \qquad (3A)$$

two-step model:

$$E + L \underset{K_c}{\rightleftharpoons} EL \underset{k_r}{\overset{k_f}{\rightleftharpoons}} EL^*$$

$$1/\tau = \frac{k_f[L]}{K_c + [L]} + k_r \qquad (3B)$$

Spectrophotometric Titrations for the Binding of Ligands to MCAD. Spectrophotometric titrations were performed either on a Perkin-Elmer Lambda-3B or on a Beckman 7400 diode array spectrophotometer. The difference spectra of the enzyme−ligand complexes were generated by subtracting the spectra of the individual components from their mixtures (after dilution corrections). The dissociation constants and the overall amplitude of the absorbance changes were obtained by analyzing the data by a complete solution of the quadratic equation (describing enzyme−ligand interaction) as elaborated by Qin and Srivastava (*15*).

Comparison of the Structural Data. The coordinates for the X-ray crystallographic structure of pig liver medium-chain acyl-CoA dehydrogenase in the absence (3MDD) and the presence of C_8-CoA (3MDE) were downloaded from Brookhaven Protein DataBank. The 3MDD and 3MDE structures have been referred to as the "apo" and "holo" structures, respectively, throughout this paper. The structural data of the enzyme were manipulated on a Silicon Graphics-O2 molecular modeling workstation, with the aid of Insight-II (98) software, developed by Molecular Simulations, Inc., as described by Srivastava and Peterson (*27*).

To show the displacement of certain amino acyl residues upon binding of C_8-CoA to the "apo" enzyme's active site, we superimposed the MDD and MDE structures (with respect to their backbones), and then created a subset of all the amino acyl residues within a 4 Å perimeter of C_8-CoA in the above structures by the aid of Insight II software. For clarity, only selected amino acyl residues of the above structures have been shown in Figure 1.

RESULTS

To quantitatively ascertain the influence of Glu-376→Gln substitution in medium-chain acyl-CoA dehydrogenase (MCAD), we compared the octanoyl-CoA-dependent reductive half-reaction and the steady-state kinetic parameters of the wild-type and E376Q mutant enzymes. Since the above mutation considerably impaired the rate of enzyme catalysis, the spectral changes during the course of the reductive half-reaction of the enzyme could be easily monitored on a diode array spectrophotometer. However, to avoid the interference of the slow "oxidase" reaction (which could be comparable to the rate of the flavin reduction), the above study was performed under strict anaerobic conditions (*21*). Figure 2 (panel A) shows the spectral changes upon mixing 12.4 μM E376Q mutant enzyme with 340 μM octanoyl-CoA via the anaerobic titration assembly (*21*). For clarity, only selected spectral traces are shown in this figure. As observed in the case of wild-type enzymes (*1*, *2*, *4*, *5*, *7*, *14*, *16*), the reductive half-reaction of the mutant enzyme is characterized by reduction of the enzyme-bound FAD at 450 nm, and the formation of the reduced enzyme-enoyl-CoA charge transfer at 568 nm. The time-resolved spectral changes are consistent with two clean isosbestic points at 363 and 505 nm, respectively.

Figure 2B shows the difference spectra, i.e., the spectra at a given time minus the first spectrum (generated from the data of Figure 2A). The data of Figure 2B reveal that the reaction of the mutant enzyme with octanoyl-CoA results in maximal increase in absorptions at 320 and 568 nm, and decrease in absorptions at 390 and 450 nm, respectively. The

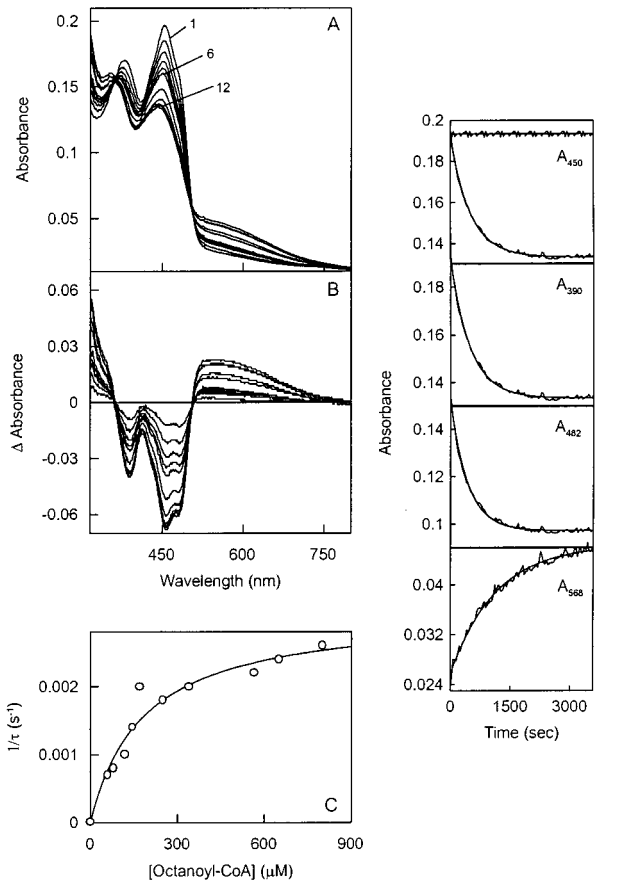

FIGURE 2: Octanoyl-CoA-dependent reductive half-reaction of Glu-376→Gln substituted enzyme. Panel A shows the spectral changes upon mixing 12.4 μM mutant enzyme with 340 μM octanoyl-CoA via anaerobic titration assembly, in the standard phosphate buffer, pH 7.6, at 25 °C. Panel B shows the difference spectra, obtained by subtracting the first spectrum from the subsequent spectra of the enzyme−octenoyl-CoA complex. For clarity, only selected spectral data are shown in panels A and B. The right-hand panels show the time course of the absorption changes at selected wavelengths. The solid smooth lines are the best fit of the data according to the single-exponential rate equation (eq 2A). The horizontal trace of the top (right-hand) panel (450 nm) is the sum of the absorptions of the reacting species (control experiment; under identical experimental condition) without the reaction. The rate constants of the kinetic traces at different wavelengths are as follows: 450 nm, 0.002 s^{-1}; 390 nm, 0.0025 s^{-1}; 482 nm, 0.0023 s^{-1}; 568 nm, 0.0018 s^{-1}. Panel C shows the octanoyl-CoA concentration dependence of the relaxation rate constant ($1/\tau$) for the reductive half-reaction, measured at 450 nm. The solid smooth line is the best fit of the data (by eq 3B) for the hyperbolic dependence of $1/\tau$ on octanoyl-CoA concentration, with the magnitudes of $1/\tau_{max}$ (relaxation rate constant at saturating concentration of octanoyl-CoA), k_r (relaxation rate constant at zero concentration of octanoyl-CoA), and K_c (the concentration of octanoyl-CoA required to achieve half of the maximum saturation) being equal to 0.0031 ± 0.0003 s^{-1}, 0.00001 s^{-1}, and 182 ± 23 μM, respectively.

right-hand panels of Figure 2 show the time slices of the spectral changes at selected wavelengths. The solid smooth lines in these panels are the best fit of the data by the first-order rate equation (eq 2A). The relaxation rate constants ($1/\tau$) derived from such analyses were found to vary between 0.0018 and 0.0025 s^{-1}, with an average value of 0.0023 s^{-1}. To ascertain whether additional absorption changes occurred prior to the observed relaxation phases, we performed a control experiment. In this experiment, the time-dependent absorption changes of the mutant enzyme (12.4 μM) and octanoyl-CoA (340 μM) were separately acquired for 60 min, and the sum of their absorptions was reconstituted at 450 nm. The horizontal (linear) trace of the top right-hand panel (A_{450}) is representative of the cumulative absorption of the reacting components (without reaction). When this trace is extrapolated (solid line) to zero time, it corresponds to the initial absorption of the reaction mixture (i.e., the zero time absorption of the observed relaxation phase at 450 nm). These data clearly suggest that no flavin reduction occurred within the mixing time (dead time) of the enzyme and octanoyl-CoA. In other words, the observed absorption change during the relaxation phase is the sole representative of the total absorption change during the course of the reductive half-reaction of the enzyme. In addition, the overall observed absorbance change at 450 nm conforms to the single (rather than double) exponential rate equation. It should be noted that the single-exponential fit of the 450 nm data yields a total amplitude of 0.059. This corresponds to about 31% reduction of the enzyme-bound FAD (by 340 μM octanoyl-CoA). In the presence of a saturating (about 900 μM) concentration of octanoyl-CoA, we calculate that about 49% of the enzyme-bound FAD is reduced. The latter value is comparable to about 48% reduction of the wild-type enzyme-bound FAD by the saturating concentration of octanoyl-CoA (*32*). These data suggest that the lack of 100% reduction of the enzyme-bound FAD is presumably because of the attainment of a finite internal equilibrium between the enzyme-bound FAD-octanoyl-CoA and $FADH_2$-octenoyl-CoA species. Such a situation is facilitated due to enormously tight binding of octenoyl-CoA to the reduced enzyme's active site (*7*).

We determined the magnitudes of the relaxation rate constants of the reductive half-reaction ($1/\tau$) of the mutant enzyme as a function of octanoyl-CoA concentration (under the pseudo-first-order conditions, [enzyme] ≪ [octanoyl-CoA]). Figure 2C shows the hyperbolic dependence of $1/\tau$ on octanoyl-CoA concentration. Such a hyperbolic profile could not be observed either with pig kidney or with recombinant human liver (wild-type) enzyme due to saturation of these enzymes at much lower concentrations of octanoyl-CoA (*4*, *5*). The solid smooth line is the best fit of the data for the hyperbolic dependence of $1/\tau$ on octanoyl-CoA concentration by eq 3B. The magnitudes of $1/\tau_{max}$ (relaxation rate constant at saturating concentration of octanoyl-CoA), k_r (relaxation rate constant at zero concentration of octanoyl-CoA), and K_c (the concentration of octanoyl-CoA required to achieve half of the maximum saturation) were found to be 0.0031 ± 0.0003 s^{-1}, 0.00001 s^{-1}, and 182 ± 23 μM, respectively.

We previously concluded that, depending upon the substrate type, MCAD catalysis was limited either by the forward rate constant of the reductive half-reaction or by the rate constant for the dissociation of the reaction product (*4*, *7*, *22*−*26*). In the case of wild-type enzyme, the octanoyl-CoA-dependent turnover rate of the enzyme has been shown to be limited by the dissociation "off-rate" of the reaction product, octenoyl-CoA (*4*, *5*, *7*). Since the E376Q mutation drastically impaired the octanoyl-CoA-dependent reductive half-reaction of the enzyme, it appeared likely that the latter step (rather than the product dissociation step) would limit the enzyme's turnover. To probe this, we compared the steady-state kinetic parameters of the wild-type and E376Q

Table 1: Steady-State Kinetic Parameters of the Wild-Type and Glu-376→Gln Mutant Enzymes[a]

enzyme type	K_m (μM)	k_{cat} (s^{-1})
wild-type MCAD	3.3 ± 0.14	17 ± 0.2
mutant MCAD	2.1 ± 0.15	0.0024 ± 0.00004

[a] Determined in 50 mM phosphate buffer, pH 7.6, containing 10% glycerol and 0.3 mM EDTA at 25 °C in the presence of 350 μM $FcPF_6$.

mutant enzymes (Table 1) with the corresponding forward rate constants (k_f ; eq 3B) of the reduction of the enzyme-bound FAD. Given that $k_f = 1/\tau_{max} - k_r$ (eq 3B and Figure 2C), the magnitude of k_f is calculated to be 0.003 s^{-1}, which is similar to the steady-state turnover rate of the mutant enzyme (0.0024 s^{-1}). Hence, unlike the wild-type enzyme (*4*, *5*, *7*, *14*, *16*), the rate-limiting step of the E376Q mutant enzyme is conformed by the rate of reduction of the enzyme-bound FAD. This appears to be achieved by impairment of the reductive half-reaction of the enzyme by about 200 000-fold upon substitution of Glu-376 by Gln.

Effect of Glu-376→Gln Substitution on the Transient Kinetics of Association of Octenoyl-CoA. Prior to undertaking a detailed kinetic comparison for the binding of octenoyl-CoA to the wild-type and mutant enzymes, we compared the spectral properties of the enzyme−octenoyl-CoA complexes. Figure 3A and Figure 3B show the spectral changes for the binding of different concentrations of octenoyl-CoA to the wild-type and E376Q mutant enzymes, respectively. The spectral data of both Figure 3A and Figure 3B are characterized by an increase in absorbance at 390 and 490 nm, and a decrease in absorbance at 370 and 440 nm, with isosbestic points at 333, 379, and 407 nm, respectively. Figure 3C compares the difference spectra of the wild-type and E376Q mutant enzyme−octenoyl-CoA complexes. These spectra were generated by subtracting the spectral contributions of both enzyme and octenoyl-CoA from the mixtures of the individual enzyme−ligand complexes. The spectral data of Figure 3C reveal that although the overall spectral features of the enzyme−octenoyl-CoA complex remain unaffected upon Glu-376→Gln substitution, there are slight changes in the spectral peaks at 394, 439, and 491 nm, respectively. We believe the origin of these changes lies in the difference in microenvironment of the enzyme's (wild-type versus E376Q mutant) active sites (*28*, *29*).

To determine the extent that Glu-376→Gln substitution alters the binding affinity of octenoyl-CoA, we performed spectrophotometric titrations for the binding of octenoyl-CoA to wild-type and mutant enzymes. The absorption maxima for the binding of octenoyl-CoA to the wild-type and mutant enzymes were determined to be 442 and 439 nm, respectively. The insets of Figure 3A and Figure 3B show the binding isotherms (at 25 °C) of the wild-type−octenoyl-CoA and E376Q−octenoyl-CoA complexes, respectively. These data were generated by titrating fixed concentrations of the wild-type and mutant enzymes with increasing concentrations of octenoyl-CoA as described previously (*15*). The solid smooth lines are the best fit of the data for the dissociation constants of the wild-type−octenoyl-CoA and E376Q mutant−octenoyl-CoA complexes as being 0.91 ± 0.01 and 0.44 ± 0.06 μM, respectively (*15*).

Utilizing the spectral signals of the individual enzyme−ligand complexes (Figure 3), we investigated the kinetics of

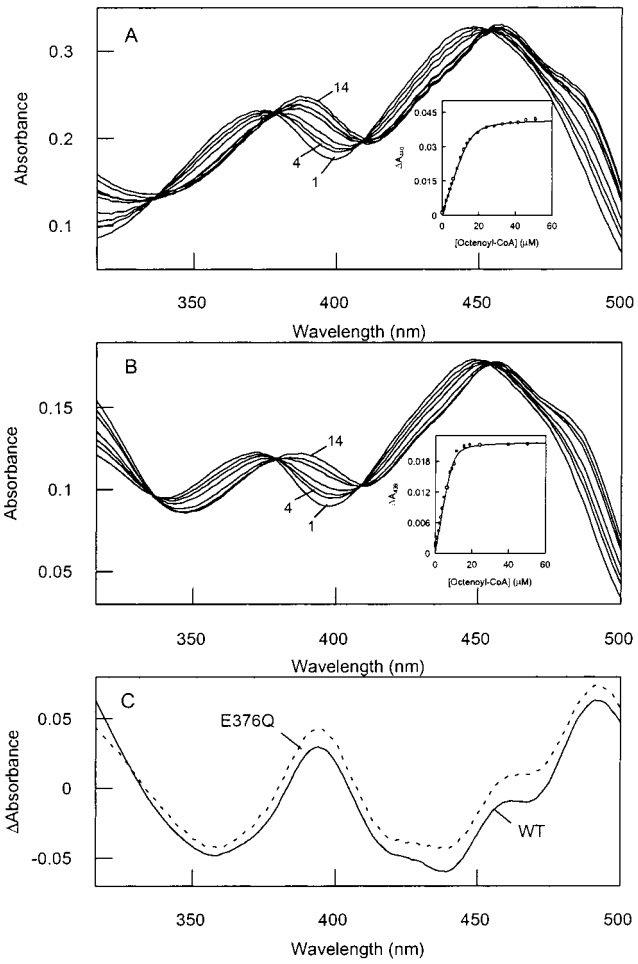

FIGURE 3: Spectral changes upon binding of octenoyl-CoA to the wild-type and Glu-376→Gln substituted enzymes. The experimental conditions were the same as in Figure 2. The concentrations of the wild-type (panel A) and mutant (panel B) enzymes were 21 and 11 μM, respectively. For clarity, only selected spectral data are shown. The insets of panels A and B show the binding isotherms for the interactions of octenoyl-CoA with the corresponding enzymes. The solid smooth lines of panels A and B are the best fit of the data according to Qin and Srivastava (*15*). The dissociation constant and the stoichiometry of the wild-type enzyme−octenoyl-CoA complex (inset of panel A) were determined to be 0.91 ± 0.10 μM and 0.9 ± 0.02, respectively. The corresponding parameters for the mutant enzyme−octenoyl-CoA complex (inset of panel B) were determined to be 0.44 ± 0.06 μM and 0.85 ± 0.03, respectively. Panel C shows the difference spectra (i.e., the spectra of the enzyme−ligand complexes minus the individual components) of the wild-type (solid line) and E376Q mutant (broken line) enzyme−octenoyl-CoA complexes. The concentrations of the enzymes and octenoyl-CoA (for the data of panel C) were 20 and 54 μM, respectively.

association of octenoyl-CoA to both wild-type and E376Q mutant enzymes. Although we previously performed the above studies involving the wild-type enzyme (*5*), for the sake of explicit comparison, we repeated these experiments involving both the enzymes. Figure 4 shows the comparative stopped-flow kinetic traces for the association of octenoyl-CoA with the wild-type (Figure 4A) and E376Q mutant (Figure 4B) enzymes under an identical experimental condition. To facilitate comparison, the kinetic traces have been normalized with respect to the enzyme concentration. This has been achieved by dividing the time course of the absorbance changes by the initial concentrations of individual enzymes. The solid smooth lines are the best fit of the data

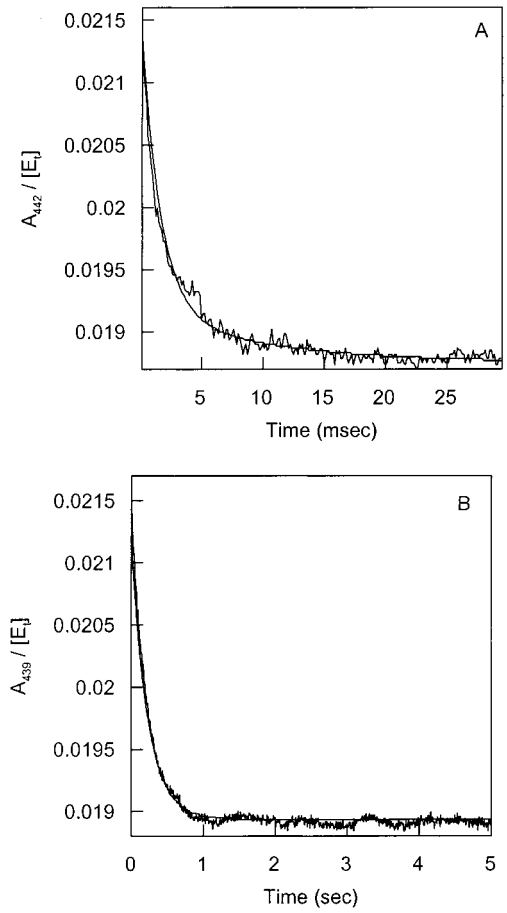

FIGURE 4: Transient kinetics for the interaction of octenoyl-CoA with wild-type and Glu-376→Gln mutant enzymes. The stopped-flow traces for the interactions of octenoyl-CoA with wild-type (442 nm) and mutant (439 nm) enzymes at 5 °C are shown in panels A and B, respectively. The solid smooth lines are the best fit of the data according to the biphasic (panel A, eq 2B) and single-exponential (panel B, eq 2A) rate equations, respectively. The after-mixing concentrations of the enzyme and octenoyl-CoA, and the derived relaxation rate constants ($1/\tau$'s) for the data of panels A and B, are summarized as follows: panel A, [wild-type enzyme] = 6 μM, [octenoyl-CoA] = 128 μM, $1/\tau_f = 676 \pm 72$ s^{-1}, $1/\tau_s = 100 \pm 9.2$ s^{-1}; panel B, [E376Q mutant enzyme] = 10 μM, [octenoyl-CoA] = 600 μM, $1/\tau = 4.56 \pm 0.4$ s^{-1}.

of Figure 4A,B by the double (eq 2B) and single (eq 2A) exponential rate equations, respectively. The fast and slow rate constants derived from the data of Figure 4A were 676 and 100 s^{-1}, respectively. The only (single-exponential) rate constant in the case of the E376Q mutant enzyme (Figure 4B) was determined to be 4.6 s^{-1}. Evidently, the slower rate constant (whose origin has been attributed to some unknown secondary process; *6*) is not apparent in the case of the mutant enzyme. However, upon comparison of the fast rate constant for the binding of octenoyl-CoA to the wild-type enzyme vis à vis the rate constant observed for the E376Q mutant enzyme, it is evident that the above mutation impairs the rate of association of octenoyl-CoA to the enzyme by about 150-fold. Hence, besides impairing the proton transfer step, during the course of the octanoyl-CoA-dependent reductive half-reaction (see Figure 2), the E376Q mutation impairs the kinetic profile for the binding of the reaction product, octenoyl-CoA, to the enzyme's active site. This result was unexpected since the carboxyl group of Glu-376 has been widely regarded to be (*exclusively*) involved in the abstraction of the α-proton from acyl-CoAs during the reductive half-reaction of the enzyme (*2*, *3*, *8*, *30*). No effect of Glu-376→Gln substitution on the kinetics of association of octenoyl-CoA to the enzyme's active site was previously envisaged. We believe the latter effect of the E376Q mutation is due to the changes in the microscopic environment of the enzyme's active site (see Discussion).

We recently reported that the electronic structural changes during the course of the enzyme−octenoyl-CoA interaction followed the same time course as the changes in the enzyme's intrinsic fluorescence, under an identical experimental condition (*6*). This observation was supportive of our hypothesis that the enzyme−octenoyl-CoA interaction involved changes in the protein conformation (*4*, *5*, *7*). Since the E376Q mutation impaired the kinetics of association of octenoyl-CoA (deduced via the absorption method) by about 150-fold (see Figure 4), it was of interest to examine whether the above mutation also impaired the rate of quenching of the intrinsic fluorescence of the enzyme. To probe this, we determined the kinetics of fluorescence changes upon mixing of 600 μM octenoyl-CoA with 4 μM E376Q mutant enzyme via the stopped-flow syringes (Figure 5A; at 5 °C). The solid smooth line is the best fit of the data according to the single-exponential rate equation (eq 2A) for the rate constant of 3.7 s^{-1}. Note that the latter value is similar to the kinetics of the electronic structural changes of the enzyme-bound FAD upon interaction with octenoyl-CoA (4.6 s^{-1}; Figure 4B). Clearly the microscopic event associated during the course of the electronic structural changes of the enzyme-bound FAD (upon interaction with octenoyl-CoA) also involves the quenching of the intrinsic fluorescence of the enzyme.

Given the above results, it was tempting to determine whether the octanoyl-CoA-dependent reductive half-reaction of the E376Q mutant enzyme also proceeded concomitant with the quenching of the intrinsic enzyme fluorescence. To ascertain this, we monitored the changes in the intrinsic protein fluorescence upon mixing 3 μM enzyme with 2 mM octanoyl-CoA (Figure 5B; at 25 °C). It should be pointed out that during this experiment, particularly on a longer time scale, the enzyme started developing a small turbidity. Although such turbidity had no influence on the absorption signal (during the course of the reductive half-reaction), it had discernible influence on the fluorescence signal. As a consequence, the fluorescence changes accompanying the octanoyl-CoA-dependent reductive half-reaction of the enzyme showed a rapid single-exponential decay phase, followed by a steady-state phase. Assuming that the latter phase was due to slow precipitation of the enzyme, it was not taken into account during the data analysis. The solid smooth line of Figure 5B is the best fit of the data according to the single-exponential rate equation (eq 2A), with a rate constant of 0.0068 s^{-1}. Note that the latter value is only about 2-fold higher than the forward rate constant (k_f) for the reductive half-reaction of the enzyme in the presence of saturating concentration of octanoyl-CoA (0.0031 ± 0.0003 s^{-1}; Figure 2B). Considering the difficulties in measuring the fluorescence changes during the course of the octanoyl-CoA-dependent reductive half-reaction (arising due to precipitation of protein), as well as the small magnitude of quenching of the intrinsic enzyme's fluorescence (*6*), we believe that the above 2-fold difference in the rate constants is not significant. However, if the above discrepancy is deemed to be signifi-

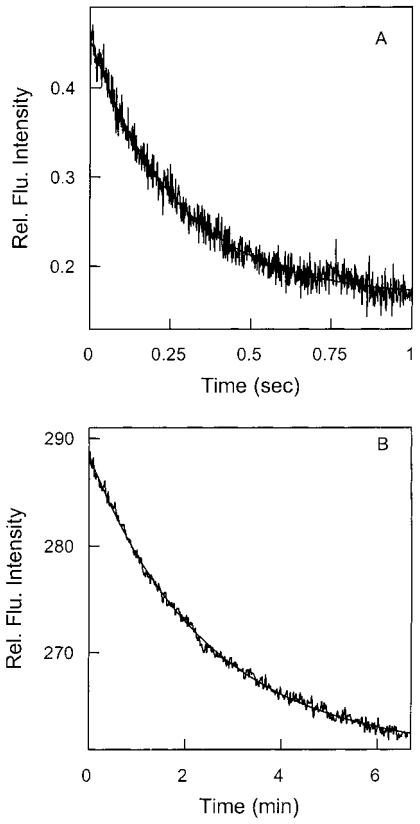

FIGURE 5: Transient kinetics for the changes in the intrinsic fluorescence of the enzyme upon interaction/reaction with C_8-CoA's. The excitation wavelength was set at 295 nm, and the emission light was passed through a cutoff filter of 335 nm. Panel A shows the stopped-flow kinetic trace for the decrease in the tryptophanyl residue's fluorescence of the Glu-376→Gln substituted enzyme upon binding octenoyl-CoA at 5 °C. The after-mixing concentrations of the enzyme and octenoyl-CoA were 6 and 400 μM, respectively. The solid smooth line is the best fit of the data according to the single-exponential rate equation (eq 2A) with a relaxation rate constant ($1/\tau$) of 3.69 ± 0.3 s^{-1}. Panel B shows the kinetic trace for the decrease in the intrinsic fluorescence of the Glu-376→Gln substituted enzyme upon reaction (reductive half-reaction) with octanoyl-CoA at 25 °C. The after-mixing concentrations of the enzyme and octanoyl-CoA were 3 μM and 2 mM, respectively. The solid smooth line is the best fit of the data according to the single-exponential rate equation with a rate constant of 0.0068 ± 0.00005 s^{-1}.

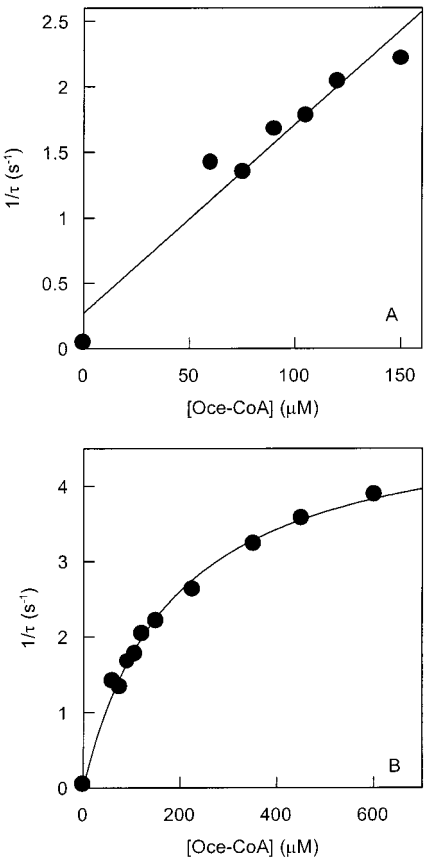

FIGURE 6: Octenoyl-CoA concentration dependence of the relaxation rate constants for the binding of the ligand to Glu-376→Gln mutant enzyme. Panels A and B represent the data (collected under pseudo-first-order conditions; [octenoyl-CoA] ≫ [enzyme]) at the lower and higher range of [octenoyl-CoA], measured at 439 nm at 5 °C. Experimental conditions are the same as mentioned in Figure 4. The after-mixing concentration of the enzyme was 7.5 μM. The data at zero concentration of octenoyl-CoA have been taken from the dissociation "off-rate" measurement. The solid smooth line of panel A is the linear regression analysis of the data (eq 3A) for the slope (k_f) and intercept (k_r) of 0.014 μM^{-1} s^{-1} and 0.272 s^{-1}, respectively. The data of panel B have been analyzed for the hyperbolic dependence of the relaxation rate constant ($1/\tau$) on octenoyl-CoA concentration (eq 3B). The solid smooth line is the best fit of the data for the relaxation rate constants at saturating concentration of octenoyl-CoA ($1/\tau_{max}$), zero concentration of octenoyl-CoA (k_r), and the concentration of octenoyl-CoA required to achieve half of the maximal saturation (K_c) being equal to 5.0 ± 0.16 s^{-1}, 0.05 ± 0.004 s^{-1}, and 184 ± 13.6 μM, respectively.

cant, its origin may be attributed to the fact that the fluorescence changes "partially" (not completely) limit the "chemistry" of flavin reduction. Hence, we propose that the E376Q mutation impaired both the rate of the octanoyl-CoA-dependent reductive half-reaction and the quenching of the intrinsic protein fluorescence by more or less the same magnitude. Therefore, as observed in the case of the enzyme−octenoyl-CoA interaction, the octanoyl-CoA-dependent reductive half-reaction of the E376Q mutant enzyme also proceeds concomitant with the quenching of the enzyme's intrinsic fluorescence.

Octenoyl-CoA Concentration Dependence of the Association Rate Constant of the Ligand with the Mutant Enzyme. To ascertain the effect of the E376Q mutation on the microscopic pathway for the enzyme−octenoyl-CoA interaction, we investigated the octenoyl-CoA concentration dependence of relaxation rate constants for the enzyme−ligand interaction (deduced via the absorption method as described in Figure 4). As shown in Figure 6A, the relaxation rate constant for the binding of octenoyl-CoA to the E376Q mutant enzyme (under pseudo-first-order conditions, [E] ≪ [octenoyl-CoA]) increases linearly up to 150 μM ligand concentration. This was in marked contrast to the "zero-order" dependence of the relaxation rate constant on octenoyl-CoA concentration in the case of wild-type enzyme (*4*, *5*). The above difference initially led to the suggestion that the binding of octenoyl-CoA to the E376Q mutant enzyme involved the "one"- (eq 3A) rather than "two"-step mechanism (eq 3B; *36*, *37*). However, we soon realized that at a much higher concentration of octenoyl-CoA, the relaxation rate constant for the association of octenoyl-CoA to the mutant enzyme exhibited a saturation profile (Figure 6B). The analysis of the data according to the two-step model (eq 3B; solid smooth line) yielded the magnitudes of K_c, $1/\tau_{max}$, and k_r as being equal to 184 μM, 5.0 s^{-1}, and 0.05 s^{-1}, respectively. Of these parameters, k_r (the dissociation

Table 2: Rate and Equilibrium Constants for the Binding of Octenoyl-CoA to the Wild-Type and Glu-376→Gln Mutant Enzymes[a]

parameters	wild-type MCAD	mutant MCAD
K_c (μM)	23.6 ± 2.9	184 ± 13.6
k_f (s^{-1})	675 ± 72	5.0 ± 0.16
k_r (s^{-1})	1.0 ± 0.01	0.00072[b]
K_d (μM)[c]	0.094	0.052

[a] For the two-step binding model of eq 1 at 5 °C. Unless noted otherwise (see below), the experiments were performed in 50 mM phosphate buffer, pH 7.6, containing 10% glycerol and 0.3 mM EDTA at 5 °C. [b] The experimentally determined k_r at 25 °C was 0.05 ± 0.004. The magnitude of k_r at 5 °C was calculated using the energy of activation (E_a) parameter of 32.3 kcal/mol. [c] Determined by spectrophotometric titration. The K_d values for the binding of octenoyl-CoA to the wild-type and mutant enzymes at 25 °C were 0.7 ± 0.1 and 0.44 ± 0.1 μM, respectively. The K_d values at 5 °C were calculated using the van't Hoff enthalpies for the binding of octenoyl-CoA to wild-type enzyme (−9.5 kcal/mol; *6*) and the mutant enzyme (−14 kcal/mol; unpublished results), respectively.

"off-rate" of the enzyme−octenoyl-CoA complex) was independently determined by the acetoacetyl-CoA displacement method (*12*). It should be noted that the magnitude of K_c for the binding of octenoyl-CoA (184 μM) is similar to that obtained for the octanoyl-CoA-dependent reductive half-reaction of the mutant enzyme (182 μM; Figure 2B), suggesting that the affinity of both octanoyl-CoA and octenoyl-CoA (within the collision complex) for the mutant enzyme's active site is remarkably the same. However, unlike the wild-type enzyme (*5*), the subsequent isomerization steps for the above diverse processes ("chemistry" versus the "electronic structural changes") differ upon Glu-376→Gln substitution.

Table 2 summarizes the microscopic parameters for the binding of octenoyl-CoA to the E376Q mutant enzyme according to the two-step binding model (eq 3B) as elaborated by Johnson et al. (*12*). For comparison, we show the corresponding parameters for the binding of octenoyl-CoA to the wild-type enzyme. It should be pointed out that except for the dissociation "off rate" of octenoyl-CoA (k_r) from the mutant enzyme (determined at 25 °C), all the microscopic parameters of Table 2 have been determined at 5 °C. So as to maintain the uniformity, we translated the magnitude of k_r from 25 to 5 °C using our previously determined energy of activation (E_a = 32.3 kcal/mol) for the dissociation of octenoyl-CoA from the mutant enzyme (K. V. Gopalan and D. K. Srivastava, unpublished results). This stratagem yielded the magnitude of k_r as being equal to 0.00072 s^{-1} at 5 °C.

We recently reported that the van't Hoff enthalpy for the binding of octenoyl-CoA to the wild-type enzyme is −9.5 kcal/mol (*6*), and we determined the van't Hoff enthalpy for the binding of octenoyl-CoA to the mutant enzyme to be −14 kcal/mol (K. V. Gopalan and D. K. Srivastava, unpublished results). Given the above van't Hoff enthalpies, we could translate the K_d values of the wild-type− and mutant enzyme−octenoyl-CoA complexes, determined at 25 °C (Figure 3C), to 5 °C. These recalculated K_d values (at 5 °C) are also summarized in Table 2.

An examination of the microscopic parameters of Table 2 lead to the conclusion that whereas E376Q mutation decreases the binding affinity of octenoyl-CoA within the collision complex (K_c) by about 8-fold, it decreases the forward (k_f) and reverse (k_r) rate constants for the isomerization of the enzyme−ligand collision complex by 135-fold and 1388-fold, respectively. Hence, the isomerization equilibrium (k_f/k_r) is, in fact, favored by 10.3-fold in the case of the E376Q mutant enzyme. Therefore, the impaired binding affinity of octenoyl-CoA within the mutant enzyme−octenoyl-CoA collision complex (8-fold) is nearly compensated by the favorable isomerization equilibrium (10.3-fold). Based on these microscopic parameters, the K_d values of the wild-type− and mutant enzyme−octenoyl-CoA complexes could be predicted ($K_d = K_c k_r/k_f$) at 5 °C to be 0.035 and 0.026 μM, respectively. These K_d values are within the 2−3-fold range of the experimentally determined values (albeit recalculated at 5 °C, using the corresponding van't Hoff enthalpies) via spectrophotometric titrations of Figure 3A,B.

DISCUSSION

The data presented herein provide a new insight into the role of the active site residue, Glu-376, of medium-chain acyl-CoA dehydrogenase (MCAD) during the course of ligand binding and catalysis. Contrary to the prevailing notion that the carboxyl group of Glu-376 is exclusively involved in abstracting the α-proton from acyl-CoA substrates during the reductive half-reaction of the enzyme (*2*, *3*, *8*), we provide evidence that it is also involved in structuring the enzyme's active site cavity and modulating the dynamics of the protein conformational changes during the course of ligand binding and catalysis. The carboxyl group of Glu-376 appears to stabilize the ground state of the enzyme−ligand collision complex, as well as the putative transition state leading to the isomerization of the above complex. The latter step has been demonstrated to be coupled to the changes in the electronic structures of the enzyme-bound FAD and the enoyl-CoA products, as well as facilitating the acyl-CoA-dependent chemical transformation step (i.e., the reductive half-reaction) of the enzyme (*4*, *5*, *7*).

It is interesting to note that the Glu-376→Gln substitution not only impairs the octanoyl-CoA-dependent reduction of the enzyme-bound FAD (during the course of the reductive half-reaction) but also impairs (by more or less the same magnitude) the concomitant changes in the intrinsic protein fluorescence of MCAD (see Figures 2 and 5). Likewise, the above mutation equally impairs both the rates of the electronic structural changes of the enzyme-bound FAD upon interaction with octenoyl-CoA and the concomitant changes in the intrinsic fluorescence of the enzyme protein (see Figures 4 and 5). Clearly, both these diverse processes (i.e., the electronic structural changes versus "chemistry") are directly (albeit independently) coupled to the changes in the microenvironment of the enzyme's active site. Such changes are ascribable to the changes in the protein conformation upon ligand binding and/or catalysis.

We previously demonstrated that in the case of both pig kidney and recombinant human liver (wild-type) enzymes, the kinetic and thermodynamic profiles for the octanoyl-CoA-dependent reductive half-reactions were precisely the same as the binding of octenoyl-CoA (*4*, *5*). However, such a marked similarity was unique for octanoyl-CoA/octenoyl-CoA as the physiological substrate/product pair of the enzyme, and it was not found with smaller chain acyl/enoyl-CoA substrate/product pairs, such as butyryl/crotonoyl-CoA,

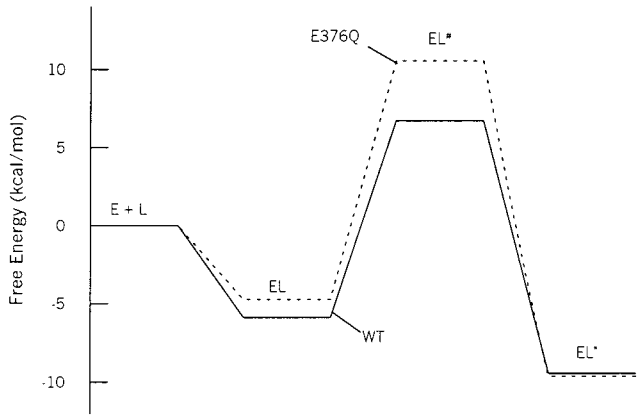

FIGURE 7: Effect of the Glu-376→Gln substitution on the free energy profile for the binding of octenoyl-CoA to the enzyme. E, L, EL, and EL* represent the free enzyme, CoA−ligand, enzyme−ligand collision complex, and enzyme−ligand isomerized complex, respectively. The free energies of the enzyme and ligand are taken as being equal to zero.

indolepropionyl/indoleacryloyl-CoA, etc (*12*, *23*, *31*). Neither was the above similarity observed with Glu-376→Asp substitution even involving octanoyl-CoA/octenoyl-CoA as the physiological substrate/product pair of the enzyme (*32*). Interestingly, a similar situation appears to prevail with the Glu-376→Gln substituted enzyme. For example, the latter mutation impairs the rate of isomerization of the enzyme−octenoyl-CoA collision complex only by150-fold, but it impairs the octanoyl-CoA-dependent reductive half-reaction by about 200 000-fold. This is presumably because the rate of proton transfer, in the case of the mutant enzyme, became significantly more impaired than the other physical processes (e.g., polarization of the carbonyl group, changes in the electronic structure of the interacting species, etc.), which are common to both octanoyl-CoA and octenoyl-CoA species. Whether the above-noted similarity is dictated by some energetic principle of the natural selection process for the evolution of MCAD and its cognate medium-chain (C_8-CoA) substrate/product pair, or it is merely a happenstance, remains to be established.

By utilizing the microscopic parameters for the binding of octenoyl-CoA to the wild-type and E376Q mutant enzyme, we could construct the comparative free energy diagrams (at 5 °C) as shown in Figure 7. The energetic profile of Figure 7 reveals that whereas the E376Q mutation destabilizes the ground-state energy of the enzyme−octenoyl-CoA collision complex by 1.1 kcal/mol, it destabilizes the subsequent transition-state energy (leading to the conversion into the isomerized complex) by 3.8 kcal/mol. Hence, the effect of the above mutation is more realized in destabilizing the transition state than the intermediary ground state. Since the above mutation has practically no influence on the ground-state energy of the isomerized enzyme−octenoyl-CoA complex, it follows that the latter complex is stabilized (vis à vis the corresponding collision complex) by about 1.3 kcal/mol.

Just how does the carboxyl group of Glu-376 modulate the energetics of the enzyme−ligand interactions and enzyme catalysis in conjunction with the dynamics of the protein conformational changes? Although there is no definitive answer to this question, we surmise that the differential electrostatic contribution of the carboxyl group of Glu-376 with the cognate enzyme's active site residues, at different stages of the enzyme−ligand interaction and enzyme catalysis, is responsible for the above effects (Figure 8). The structural data of the enzyme reveal that the carboxyl group of Glu-376 is in the closest vicinity to the isoalloxazine ring of FAD in the "apo" (ligand free) structure (Figure 1). Given the pK_a of the carboxyl group of Glu-376 as being equal to 6.0 (*34*), it is expected to be fully negatively charged at the experimental pH of 7.6. On the other hand, due to strong hydrogen bonding between selected groups of the isoalloxazine ring [viz., C(4)═O, C(2)═O, and N1] of FAD with the complementary amino acyl side chain residues of MCAD (*9*−*11*), the enzyme-bound isoalloxazine ring becomes electron-deficient (*43*), and thus exhibits cationic (partially positively charged) properties. Besides tight interaction of anionic ligands (e.g., acetoacetyl-CoA, CoA-persulfide, etc.) with the oxidized enzyme (MCAD-FAD), coupled with the formation of the "colored" charge-transfer bands (*1*−*3*), the evidence for the cationic nature of the isoalloxazine ring comes from both NMR (*44*) and resonance Raman spectroscopy (*45*). Hence, the negatively charged carboxyl group of Glu-376 is likely to interact (electrostatically) with the partially positively charged isoalloxazine ring of the enzyme-bound FAD. We propose that such an interaction is responsible for maintaining the enzyme's active site cavity, which is just apropos for the complementary interaction of the C_8-CoA ligands, leading to the formation of the enzyme−ligand collision complex. Since the Glu-376→Gln substitution eliminates the above negative charge, the enzyme's active site cavity becomes somewhat unstructured, resulting in a weaker interaction of the C_8-CoA ligands (8-fold in the case of octenoyl-CoA) in the corresponding collision complexes. As demonstrated previously (*27*), the enzyme−ligand isomerization step (eq 1) accompanies polarization of the carbonyl group of the CoA-ligands (due to the formation of strong hydrogen bonds between the carbonyl oxygen of the ligands and the 2′-ribityl hydroxyl group of FAD and the main chain amide nitrogen of Glu-376; *10*, *11*), and thus generates a partial positive charge at the carbonyl carbon atom of the ligand. At the same time, the carboxyl group of Glu-376 swings away (by about 1−4 Å) from its original position in the "apo" enzyme (Figure 1). Now, the carboxyl group in its new position has potential to interact with the partially positively charged carbonyl carbon atom of C_8-CoA, precluding favorable juxtaposition of the isoalloxazine ring of FAD and the cognate regions of the C_8-CoA moiety. Such a scenario would obviate "maximal" polarization of the carbonyl group of C_8-CoA within the corresponding isomerized complex. Hence, as observed experimentally (see Figure 7), the carboxyl group of Glu-376 is responsible for stabilizing the ground state of the enzyme−ligand collision complex in preference to that of the isomerized complex. Since the Glu-376→Gln substitution eliminates the negative charge, the above constraints are minimized, resulting in the stabilization of the ground state of the enzyme−ligand isomerized complex with respect to the preceding collision complex. Such a preferential stabilization is manifested in the form of marked spectral changes upon interaction of chromophoric ligands to the mutant vis à vis the wild-type enzyme's active site, and since the overall equilibrium in the case of Glu-376→Gln substitution is significantly favored toward the isomerized complex, no further effect of pH on

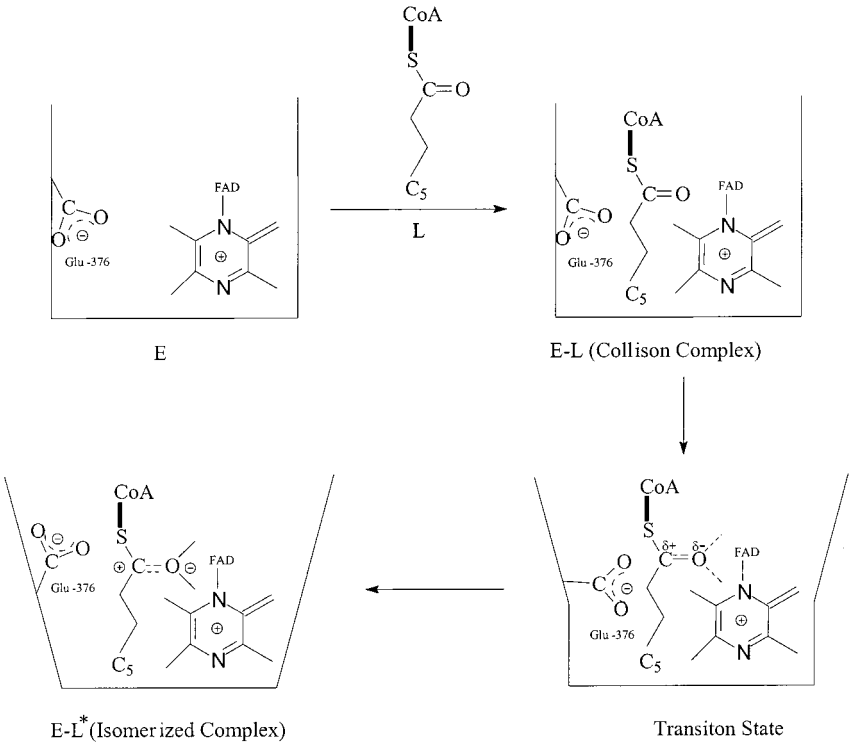

FIGURE 8: Proposed sequence of events during the course of C_8-CoA binding to the enzyme's active site. The electrostatic interaction between the carboxyl group of Glu-376 and the partially positively charged isoalloxazine ring of FAD maintains the enzyme active site cavity, which is just apropos for accommodating C_8-CoA (top left). The structure of the enzyme as well as the ligand remains unchanged within the enzyme−ligand collision complex (top, right). The conversion of the enzyme−ligand collision complex to the isomerized complex involves polarization of the carbonyl group of C_8-CoA, which proceeds concomitant with the changes in the protein conformation. The carboxyl group of Glu-376 stabilizes the partially positively charged carbonyl group of the ligand in the transition state (bottom, right), as well as in the enzyme−ligand isomerized complex (vis à vis the corresponding collision complex; bottom left).

the magnitudes of the spectral changes are evident (*28*, and our unpublished results).

In accounting for the effect of Glu-376→Gln substitution on the forward (k_f) and reverse (k_r) rate constants of the enzyme−ligand isomerization process, we note that the polarization of the carbonyl group of octenoyl-CoA would generate a partial positive charge in the transition state, which would be effectively stabilized by the carboxyl group of Glu-376. Since Glu-376→Gln substitution eliminates such a negative charge, the transition state, flanking between the enzyme−ligand collision and isomerized complexes, has a higher energy barrier.

We believe that the structure−function relationship derived from the binding of octenoyl-CoA to the enzyme's active site is applicable to the reductive half-reaction of the enzyme utilizing octanoyl-CoA as a physiological substrate, since both these processes involve polarization of the carbonyl groups of these CoA-derivatives, and proceed via similar microscopic pathways (*4*−*6*). However, due to an added involvement of the proton transfer step, the influence of Glu-376→Gln substitution on the octanoyl-CoA-dependent reductive half-reaction is more profoundly realized than that obtained during the enzyme−octenoyl-CoA interaction. In this regard, it should be pointed out that even if Gln-376 had potential to abstract the α-proton from the octanoyl-CoA substrate as efficiently as Glu-376, it would not have supported efficient catalysis due to diminution in the dissociation "off-rate" of the reaction product. Hence, besides serving as an efficient active site base, the carboxyl group of Glu-376 is intimately involved in controlling the binding and reactivity of ligands via modulating the dynamics of the protein conformational changes, which are coupled to the changes in the electrostatic interaction among cognate enzyme-bound ligands.

REFERENCES

1. Beinert, H. (1963) *Enzymes, 2nd Ed. 7*, 447−466.
2. Engel, P. C. (1990) in *Chemistry and Biochemistry of Flavoenzymes* (Muller, F., Ed.) Vol. III, pp 597−655, CRC Press, Inc., London.
3. Thorpe, C., and Kim, J.-J. P. (1995) *FASEB J. 9*, 718−725.
4. Kumar, N. R., and Srivastava, D. K. (1994) *Biochemistry 33*, 8833−8841.
5. Peterson, K. L., Sergienko, E. E., Wu, Y., Kumar, N. R., Strauss, A. W., Oleson, A. E., Muhonen, W. W., Shabb, J. B., and Srivastava, D. K. (1995) *Biochemistry 34*, 14942−14953.
6. Peterson, K. M., Gopalan, K. V., and Srivastava, D. K. (2000) *Biochemistry 39*, 12659−12670.
7. Kumar, N. R., and Srivastava, D. K. (1995) *Biochemistry 34*, 9434−9443.
8. Bross, P., Engst, S., Strauss, A. W., Kelly, D. P., Rasched, I., and Ghisla, S. (1990) *J. Biol. Chem. 265*, 7116−7119.
9. Kim, J. J, and Wu, J. (1988) *Proc. Natl. Acad. Sci. U.S.A. 85*, 6677−6681.
10. Kim, J.-J. P., Wang, M., and Paschke, R. (1993) *Proc. Natl. Acad. Sci. U.S.A. 90*, 7523−7527.
11. Lee, H. J., Wang, M., Paschke, R., Nandy, A., Ghisla, S., and Kim, J. J. (1996) *Biochemistry 35*, 12412−12420.
12. Johnson, J. K., Wang, Z. X., and Srivastava, D. K. (1992) *Biochemistry 31*, 10564−10575.
13. Peterson, K. M., and Srivastava, D. K. (2000) *Biochemistry 39*, 12678−10687.
14. Srivastava, D. K., Kumar, N. R., and Peterson, K. L. (1995) *Biochemistry 34*, 4625−4632.

15. Qin, L., and Srivastava, D. K. (1998) *Biochemistry 37*, 3499−3508.
16. Johnson, J. K., and Srivastava, D. K. (1993) *Biochemistry 32*, 8004−8013.
17. Lehman, T. C., Hale, D. E., Bhala, A., and Thorpe, C. (1990) *Anal. Biochem. 186*, 280−284.
18. Thorpe, C., Matthews, R. G., and Williams, C. W., Jr. (1979) *Biochemistry 18*, 331−337.
19. Bernert, J. T., and Sprecher, H. (1977) *J. Biol. Chem. 252*, 6737−6744.
20. Dauber-Osguthorpe, P., Roberts, V. A., Osguthorpe, D. J., Wolff, J., Genest, M., and Hagler, A. T. (1988) *Proteins: Struct., Funct., Genet. 4*, 31−47.
21. Williams, C. H., Arscott, L. D., Matthews, R. G., Thorpe, C., and Wilkinson, K. D. (1979) *Methods Enzymol.*, 62185−62198.
22. Johnson, J. K., Kumar, N. R., and Srivastava, D. K. (1993) *Biochemistry 32*, 11575−11585.
23. Johnson, J. K. (1994) Ph.D. Dissertation, North Dakota State University, Fargo, ND.
24. Kumar, N. R. (1997) Ph.D. Dissertation, North Dakota State University, Fargo, ND.
25. Reinsch, J., Rojas, C., and McFarland, J. T. (1983) *Arch. Biochem. Biophys. 227*, 21−30.
26. Schopfer, L. M., Massey, V., Ghisla, S., and Thorpe, C. (1988) *Biochemistry 27*, 6599.
27. Srivastava, D. K., and Peterson, K. L. (1998) *Biochemisry 37*, 8446−8456.
28. Rudik, I., Ghisla, S., and Thorpe, C. (1998) *Biochemistry 37*, 8437−8445.
29. Rudik, I., Bell, A., Tonge, P. J., and Thorpe, C. (2000) *Biochemistry 39*, 92−101.
30. Powell, P. J., and Thorpe, C. (1988) *Biochemistry 27*, 8022−8028.
31. Peterson, K. L., and Srivastava, D. K. (1997) *Biochem. J. 325*, 751−760.
32. Peterson, K. L., Galitz, D. S., and Srivastava, D. K. (1998) *Biochemistry 37*, 1697−1705.
33. Srivastava, D. K., Wang, S., and Peterson, K. L. (1997) *Biochemistry 36*, 6359−6366.
34. Vock, P., Engst, S., Eder, M., and Ghisla, S. (1998) *Biochemistry 37*, 1848−1860.
35. Peterson, K. M., Gopalan, K. V., Nandy, A., and Srivastava, D. K. (2001) *Protein Sci. 10*, 1822−1834.
36. Strickland, S., Palmer, G., and Massey, V. (1975) *J. Biol. Chem. 250*, 4048−4052.
37. Bernasconi, C. F. (1976) *Relaxation Kinetics*, Academic Press, New York.
38. Xu, Y., Nenortas, E., and Beckett, D. (1995) *Biochemistry 34*, 16624−16631.
39. Huang, Z. F., Wun, T. C., and Broze, G. J. (1993) *J. Biol. Chem. 268*, 26950−26955.
40. Gutfreund, H. (1987) *Biophys. Chem. 26*, 117−121.
41. Muh, U., Williams, C. H., and Massey, V. (1994) *J. Biol. Chem. 269*, 7989−7993.
42. Sambrook, J., Fritsch, E., and Maniatis, T. (1989) in *Molecular cloning*: *A Laboratory manual*, 2nd ed., Cold Spring Harbor Laboratory, Cold Spring Harbor, NY.
43. Ghisla, S., and Massey, V. (1989) *Eur. J. Biochem. 181*, 1−17.
44. Miura, R., Nishina, Y., Sato, K., Fujii, S., Kuroda, K., and Shiga, K. (1993) *J. Biochem. 113*, 106−113.
45. Nishina, Y., Sato, K., Shiga, K., Fugi, S., Kiyo, K., and Miura, R. (1992) *J. Biochem. 111*, 699−706.

BI011676P